A method for efficient and robust estimation of low noise, high dynamic range B0 maps

Joseph Dagher[1], Ali Bilgin[2], Timothy Reese[3], Georges El Fakhri[1]

[1]Nuclear Medicine and Molecular Imaging, Department of Radiology, Massachusetts General Hospital, Harvard Medical School, Boston, MA, United States; [2]Departments of Biomedical Engineering and, Electrical and Computer Engineering, University of Arizona, Tucson, AZ, United States; [3]Athinoula A. Martinos Center for Biomedical Imaging, Department of Radiology, Massachusetts General Hospital, Harvard Medical School, Boston, MA, United States

Introduction: Accurate estimation of field inhomogeneity maps is of critical importance in numerous MR applications, including EPI distortion correction, fat-water separation, MR spectroscopy, etc. The usual method is to estimate the field map from multiple scans of the object acquired at different echo times [1-3]. A fundamental accuracy-robustness trade-off exists in such multi-echo field map estimation techniques: a large difference between the echo times reduces the maximum detectable inhomogeneity value while a short echo time difference yields unreliable measurements with high variance. In this work, we present a practical acquisition method, and a corresponding reconstruction algorithm, which yield field map estimates that are not subject to this fundamental accuracy-robustness trade-off.

Theory and Methods: Consider the spatial-domain MR signal obtained with a Gradient Echo (GRE) pulse sequence at different echo times. Using the conjugate phase method, the phase difference between the signals at echo times TE_i and TE_j can be written as:

$$\psi_{i,j}(x,y) = 2\pi\gamma\Delta B(x,y)\Delta\mathrm{TE}_{i,j} + \Delta\boldsymbol{\Omega}_{i,j}(x,y) + 2\pi n_{i,j}(x,y), \quad (1)$$

where $\Delta B(x,y)$ is the field inhomogeneity map, $\Delta\boldsymbol{\Omega}_{i,j}(x,y)$ is a random variable denoting the phase contribution of the additive noise and $n_{i,j}(x,y)$ is a phase wrapping integer which forces $\psi_{i,j}(x,y)$ to be in the range of $[-\pi,\pi]$. The estimated field map derived from (1) can thus be written as:

$$\widehat{\Delta B}_{i,j}(x,y) = \Delta B(x,y) + \frac{n_{i,j}(x,y) + {}^{\Delta\boldsymbol{\Omega}_{i,j}(x,y)}/_{2\pi}}{\gamma\Delta\mathrm{TE}_{i,j}}. \quad (2)$$

Ignoring noise momentarily, it is clear from (2) that the computed estimate $\widehat{\Delta B}_{i,j}(x,y)$ deviates from the true value $\Delta B(x,y)$ by ${}^{n_{i,j}(x,y)}/_{\gamma\Delta\mathrm{TE}_{i,j}}$. Because $n_{i,j}(x,y)$ is unknown, the solution set consists of a grid of discrete points, uniformly spaced by $\frac{1}{\gamma\Delta\mathrm{TE}_{i,j}}$. Obviously, the solution we seek corresponds to $n_{i,j}(x,y)=0$. The main challenge is that the location of such a solution on this grid is not known *apriori*. We claim that this ambiguity could be resolved with a third acquisition. Performing a similar analysis using echo times TE_i and TE_k, we readily see that the solution set from this acquisition pair is a grid of points now separated by $\frac{1}{\gamma\Delta\mathrm{TE}_{i,k}}$. With a careful choice of $\Delta\mathrm{TE}_{i,j}$ and $\Delta\mathrm{TE}_{i,k}$, the only overlapping points between these 2 grids is the solution that corresponds to $n_{i,j}(x,y) = n_{i,k}(x,y) = 0$. This novel observation constitutes the basis of our proposed method, Grids for Robust and Efficient Estimation of Field-maps (GREEF). Extending this framework to account for noise requires the consideration of a grid of line segments instead of a grid of points. The lengths of the segments are determined by the noise statistics and represent the confidence interval in which the estimated field map values $\widehat{\Delta B}_{i,j}(x,y)$ and $\widehat{\Delta B}_{i,k}(x,y)$ reside. Furthermore, it is possible to optimally select the echo times such that the overlap between the two grid of segments is minimized. We summarize the full GREEF method as follows. (i) Given a model of noise statistics as a function of echo time, we determine the optimal TE_i, TE_j and TE_k which would guarantee both, (a) maximum separation between segments $\forall(n_{i,j}(x,y), n_{i,k}(x,y)) \neq 0$ over an arbitrary field inhomogeneity spectral range of interest (this removes the need for phase unwrapping) and, (b) minimum variance estimation of the original inhomogeneity value from segments corresponding to $n_{i,j}(x,y) = n_{i,k}(x,y) = 0$ (this reduces the variance of the estimates). We formulated this problem as a numerical programming routine solved with adaptive Simulated Annealing. This is run once, offline, prior to acquisition. (ii) We acquire 3 GRE images at the prescribed echo times. (iii) In post-processing, for each pixel (x,y), we populate the two grids according to (2) and, determine the most likely overlapping segment. We then combine the measurements in that segment, pixel-by-pixel, using minimum Mean Squared Error (MSE) methods. No further post-processing is performed on the images.

Results: Data were collected on a 3T scanner using a cylindrical water phantom containing oil and air running in tubes along its long axis. At 3T, the inhomogeneity is expected to be around -430 Hz in the oil regions. This implies that the shortest echo time difference between the echoes, $\Delta\mathrm{TE}_{\mathrm{min}}$, needed in order to correctly estimate field map values in this range can not exceed 1.16ms. The slice thickness was set to 0.8mm. We compare the performance of our algorithm to two representative methods from the literature. The first method uses 14 echoes to compute the slope [2] while the second method approximates it using only 3 echoes [1]. Similar to our approach, the method in [1] has a short acquisition time. We first report the results using these methods when $\Delta\mathrm{TE}_{\mathrm{min}}$ is larger than 1.16ms. Figure 1a shows the resulting field map obtained using the 14-echo method, with the echoes incorrectly chosen to be 1.2ms apart, between 6 and 21.6ms. Figure 1b shows the field map obtained with the 3-point method, with $\mathrm{TE}_{3\mathrm{pt}} = 6, 7.2, 15$ms. As can be seen, despite generating low noise, smooth estimates inside water, both methods failed to yield correct field map values inside oil (arrows in Figure 1b), as expected. We attempt to remedy this situation by decreasing $\Delta\mathrm{TE}_{\mathrm{min}}$. The result is shown in Figure 1c and Figure 1d for the 14-point ($\mathrm{TE}_{14\mathrm{pt}} = 6, 6.8, 7.6, ..., 17.7$ms) and 3-point methods ($\mathrm{TE}_{3\mathrm{pt}} = 6, 6.9, 15$ms), respectively. Despite observing an improvement in the estimate inside oil, both methods now yield high variance noisy estimates. The result obtained using the proposed GREEF method is shown in Figure 1e. The vast improvement in field map quality as compared to the other methods is clearly visible. We can see that GREEF was able to estimate the field map efficiently and robustly, both inside water and oil. The echo times used by GREEF are $\mathrm{TE}_i = 10.3$ms, $\mathrm{TE}_j = 13.3$ms and $\mathrm{TE}_k = 8.3$ms. These values were chosen by the optimizer to yield efficient and robust results over an inhomogeneity range of $[-480, 480]$Hz for slices with a minimum T2 of 100ms and a minimum SNR of 6 (15dB). The resulting grids guarantee a confidence value of ± 10Hz in the field map estimate at an SNR of 6. It is worth emphasizing that GREEF was able to correctly disambiguate the field maps values without phase unwrapping despite the fact that $\Delta\mathrm{TE}_{\mathrm{min}}$ in data acquisition was longer than 1.16ms. Removing the upper limit on $\Delta\mathrm{TE}_{\mathrm{min}}$ enables our method to obtain robust high quality estimates across an arbitrary spectral range of interest. This demonstrates GREEF's capability in overcoming the noise-high dynamic range trade-off in field map estimation. **Conclusion:** We presented a method for estimating field maps over a large dynamic range which (i) does not require the use of short echo time differences (ii) produces robust estimates and, (iii) requires no phase unwrapping.

Acknowledgement: NIH grant T32EB013180.

References: [1] Aksit P, Derbyshire JA, Prince JL, ISBI 2007, 141-144. [2] Reber PJ, Wong EC, Buxton RB, Frank LR, MRM 1998; 39:328-330. [3] Funai AK et. al., IEEE Trans Med Imaging 2008; 10:1484-1494.

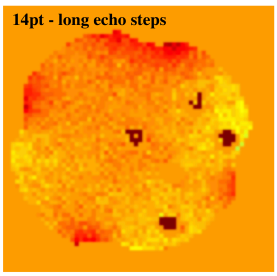

Fig. 1a

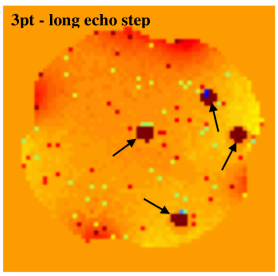

Fig. 1b

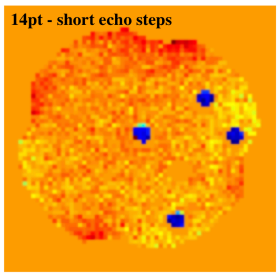

Fig. 1c

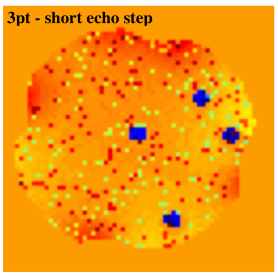

Fig. 1d

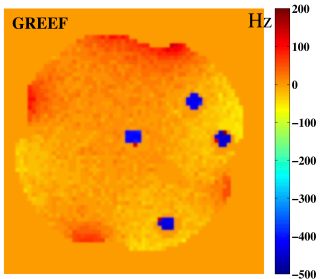

Fig. 1e